

DEVELOPMENT AND SIZING OF A MULTICRITERION FACADE ELEMENT THROUGH DIFFERENT LUMINOUS, THERMAL AND AIRFLOW TOOLS

Virginie Meunier¹ and Marjorie Musy¹

¹Cerma-UMR 1563, Ecole d'Architecture de Nantes, rue Massenet
BP 81931, 44319 Nantes cedex 3 – France

Email : prénom.nom@cerma.archi.fr

ABSTRACT

People that work in office buildings have new needs in terms of comfort within their work place. We suggest to develop a multicriteria office cell façade, allowing to control luminous, thermal and airflow parameters. It will be controlled to offer global comfort to the office cells occupants. Various simulations tools were used to optimize the dimensioning of the envelope components (solar protection (slats and electrochromic protection), to choose materials (nature and characteristic of the glazings) and to establish a natural ventilation strategy through the wall element (ventilation scenario choice, airflow patterns, and ventilation areas). This study was carried out within the frame of a Ph.D. supported by the Ademe agency and an industrial partner, in order to develop a multicriteria wall element leading to the making of a demonstrator.

INTRODUCTION

In spite of the improvement of comfort condition requirements, architects do not systematically use modern tools to check the performances of the architectural elements they conceive. Due to the absence of real control of the size of these systems, numerous sunshades do not fulfill their purpose as initially planned. This can induce discomfort for the users. It is thus quite necessary that architects check carefully the efficiency of the new systems they conceive. In the present work, after a presentation of the multicriteria office cell façade, the luminous, thermal and airflow parameters of which will be controlled, we explain the methods and tools we used to evaluate the lighting, thermal and airflow performances of this envelope. We show how the numerical tools made it possible to optimize the sizing up of the different architectural elements of the envelope. At last, we present the results of the simulations that allow to evaluate the different parameters.

STUDIED SYSTEM

The office cell envelope is a double skin. There are two series of mobile slats outside the double skin, one inside the office and the other outside and an

electrochromic glazing. All these elements allow for luminous and thermo-aerolic comfort during all year long. The slats system is neither a Venetian blind nor a rigid sunshade, since it is profiled and mobile (see below). The geometry of the cell envelope is shown in Figure 1.

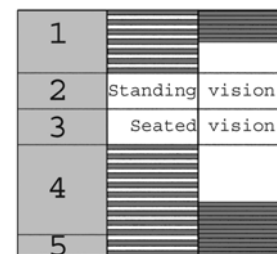


Figure 1: Geometry of the cell envelope. The first column describes the five elements of the wall, the second one gives the configurations when the slats are open, and last one when they are closed.

The double skin, a single-story interstitial space, allows for the ventilation (a natural one) of the office cell. Two ventilation strategies were retained: one for fall/winter time and the other for spring/summer time. In fall/winter, fresh air allowed in from outside enters the interstitial space of story 1 (Figure 2) and gets pre-heated during a certain time (this is the so-called pre-heating phase). This warmer air then enters the lower part of the cell room situated above it (story 2). This principle repeats itself up to the top of the office building. The pre-heated air enters the lower part of each cell room thanks to the depression created during the opening of a trap located at the bottom of the double skin. This is the so-called ventilation phase. A cycle corresponds to the two above one (pre-heating and ventilation). For the fall/winter period, the hygienic flow rate is ensured on one cycle. The chimney stack which serves several building levels then extracts the air of the room. Figure 2 and Figure 3 show the system geometry (cell + double skin + chimney) and the location of the ventilation air inlet and exhaust openings for fall/winter and spring/summer periods. For the spring/summer period, the double skin works as shown on Figure 3: There are two air flows, the first one directly entering the cell room through its bottom and escaping through the chimney (this is just the hygienic

ventilation) the second one (more important) flowing within the double skin and limiting the heating of the two glazing panels.

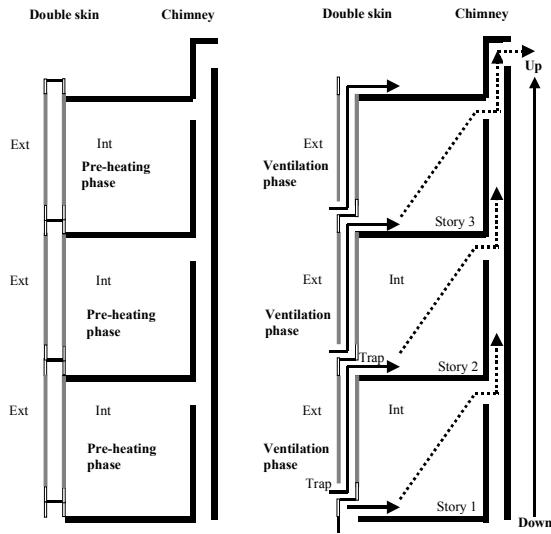


Figure 2 : Ventilation strategy – fall/winter period.

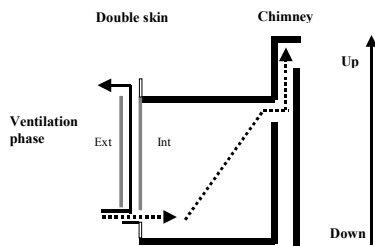


Figure 3: Ventilation strategy – spring/summer period.

METHODOLOGY

There is no available simulation tool to evaluate simultaneously the interactions existing between the comfort parameters [Meunier, 2001]. It is for this reason that we use a specific tool for each one of them, except for thermal and airflow phenomena that, in our case, cannot be considered separately.

To handle the solar constraints of the office cell [Meunier, 2002], we used the SVR software (Sun, Visibility, & Reflection) that is based on an inverse simulation method [Houpert, 2002]. This interface can be used from AutoCAD 2000®, a software widely found in architect agencies. Only the direct solar rays will be taken into account [Meunier, 2002]. For a given architectural constraint, this inverse approach consists in visualizing all the sunrays in a volume (constraint volume). In a second step, the use of this volume allows to size up the openings and the solar screens. The inverse simulation method permits the optimization of the solar protection size. In order to evaluate the influence of the solar protection shape [Meunier, 2002] on the lighting of the working surface, the Solene [Groleau, 2000] software was used. Solene allows simulating the solar and

luminous phenomena integrating sky models and inter-reflections.

To predict thermal and ventilation performances of the envelope, we developed a specific model. This work has been done in the SPARK modular environment [Lawrence Berkley Laboratory] that automates writing code for systems of non-linear equations. To each equation is associated a *class* while a *macro-class* gathers sets of equations. *Classes* and *macro-classes* are instantiated (objects and macro-objects) as many times as necessary for the formulation of the problem. Once objects and macro-objects are generated (this is done automatically using the SPARK tool sparksym [Lawrence Berkley Laboratory], it only remains to the user to connect them together. SPARK reconstitutes the equations system and solves it. Our work consisted in creating *atomic classes* corresponding to each individual equation and combining (usually by hand) them into *macro-classes* that correspond to “modules” and “interfaces”. *Classes* are stored in a model library for later use. After instantiation, the “module” and “interface” objects were linked, i.e., the variables shared by objects are identified. At last, we identified the variables that will be either input or calculated data. Otherwise, the ability of SPARK to permute data and results has widely been used to evaluate the sensitivity of the system efficiency to the sizing up parameters taken separately or together. Having devoted our tool to a specific application, we could start from a simple problem making coarse assumptions and enrich it by adding equations allowing defining the physical phenomena more finely. The specific model we built allows the dimensioning of the various wall components: single-story interstitial space thickness, areas of natural ventilation devices, choice of materials characteristics....).

MODELLING AND SIMULATIONS

It should be noted that the office cell frontage was chosen as to be west oriented To guarantee the wall element efficiency in term of energy, we chose the most unfavorable conditions for simulations, that is December 21rst from 3pm to 4pm, a period for which the solar radiation energy is about 130Wh/m².

Optimization of the sunshade size

We optimized the wall element with regard to the solar and luminous constraints by using SVR interface and the Solene software [Meunier, 2002].

The simulations made with the SVR interface for different periods of the year and answering the constraint “working plane protected” for the considered period (Figure 5) [For fall/winter: in December from 12.30pm to 3pm, in January/November from 12.30pm to 3.30pm, in February/October from 12.30pm to 4pm and in

March/September from 12.30pm to 5pm. For spring/summer: in March/September from 12.30pm to 4pm and in April/August, May/July and June from 12.30pm to 5pm] show that the optimization of the strip size takes place in all the set directions (Figure 4).

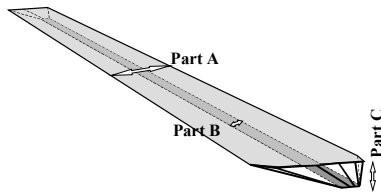


Figure 4: Slat optimal shape having a given thickness C. The A portion (upper part) of the strip alone gives the same protection than the B (lower part) and C (thickness) portions together.

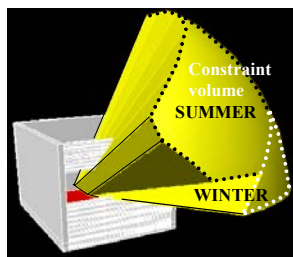


Figure 5: Two constraint volumes (for fall/winter period and spring/summer period) – office cell working plane protected for fall/winter period and spring/summer period.

The sizing up of the slats is made by considering essentially their width since this one has a considerable influence on the visibility constraint. The optimization was made only for the fall/winter and spring/summer times (Figure 6).

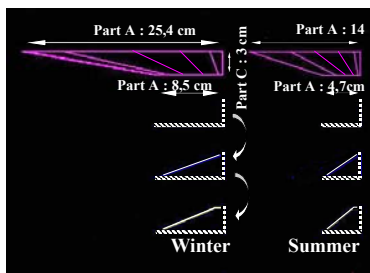


Figure 6: Slats optimal width and fall/winter and spring/summer options of slats shapes.

The slats configuration corresponds to slats thickness of 3cm and to spacing between them of 1.5cm. Let us consider the lower portion of the slat: to ensure a complete protection, its optimal width is 8.5cm in spring/summer and 4.7cm in fall/winter (Figure 6).

Evaluation of the slats dimensioning on the daylighting of the office cell working plane

We evaluated the impact of the slats form and their contribution on the day-lighting of the office cell working plane. The slats reflections represent between 9.8 and 17.8% of the whole lighting on the working plane (Figure 7).

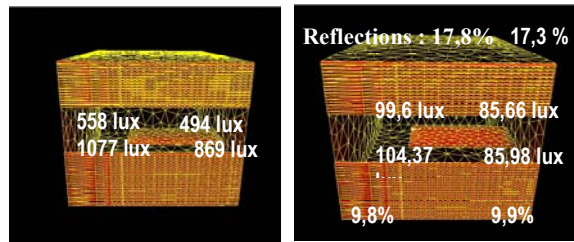


Figure 7: a) Lighting of the office cell working plane considering the walls and the slats reflections, b) Lighting of the office cell working plane due to the slats reflections.

Optimization of electrochromic protection size

The transparent part of the envelope without the slats, which allows an outside view, gives a sunspot on the working plane. To counter this inconvenience and avoid any dazzling discomfort, we suggest using, for this part of the glass panel, a sun-controlled electrochromic display. The effects of the phenomenon on the transmission can be modulated since it is proportional to the electric quantity injected into the system. A new way of partitioning the glass is created. We suggest splitting up the electrochromic area into several smaller surfaces in order to darken only these regions necessary to the protection of the working plane. The optimal colored zones of the electrochromic area were determined with the SVR interface (Figure 8). The value of the light absorption coefficient being rather high in the colored state, we made some simulations allowing to have a more accurate determination of the electrochromic colored zones for one hour for different months of the year (Figure 8).

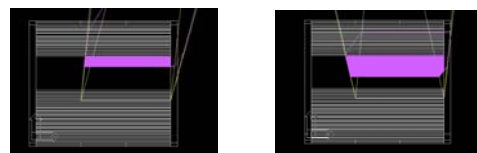


Figure 8: Electrochromic protection in the colored state during the day – working plane protected on June 21 from 3pm to 4pm (on the left) and on June 21 from 4pm to 5pm (on the right).

The SVR interface allowed us optimizing the sizing up of the different architectural elements of the glass office cell façade: shape of the slats, electrochromic protection located in the area that is devoid of them.

Thermal and ventilation behavior of the envelope

To build a model in the SPARK modular environment, we write set of equations that describe the double skin thermal behavior.

Double skin thermal behavior: basic model

The model was written for fall/winter time, knowing that for spring/summer, no pre-heating will have to be considered. We write that the hygienic flow rate must

be achieved on average. So, the ventilation flow rate, the pre-heating phase and the ventilation phase and hygienic flow rate are connected. For the fall/winter period, the ventilation scenario (ventilation phase + pre-heating phase) must follow the equation:

$$Q_{\text{vid}} = \left(\frac{t_{\text{ch}} + t_{\text{vid}}}{t_{\text{vid}}} \right) Q_{\text{hyg}} \quad (1)$$

The short-wave radiative flux that arrives on the interior side of the exterior glass panel, $\varphi_{\text{CLO_fe}}$, and the one arriving on the exterior side of the interior glass panel, $\varphi_{\text{CLO_fi}}$ depends on the glazing characteristics and on the short-wave radiative flux arriving on the device:

$$\varphi_{\text{CLO_fe}} = \alpha_{\text{CLO_e}} \cdot \tau_e \cdot \rho_i \cdot E_i \cdot \left(\frac{1}{1 - \rho_i \cdot \rho_e} \right) \quad (2)$$

$$\varphi_{\text{CLO_fi}} = \alpha_{\text{CLO_i}} \cdot \tau_e \cdot E_i \cdot \left(\frac{1}{1 - \rho_i \cdot \rho_e} \right) \quad (3)$$

The following equation represents the energy flux balance applied to the exterior face of the double skin, linking short- and long-wave radiative fluxes absorbed by the exterior glazing, conductive and convective fluxes:

$$h_{\text{ext}} (T_{\text{ext}} - T_{\text{p_ext}}) + \alpha_{\text{CLO_ext}} E_i + \alpha_{\text{GLO_ext}} \varphi_{\text{GLO_ext}} = \frac{\lambda_e}{e_e} \cdot (T_{\text{p_ext}} - T_{\text{p_fe}}) \quad (4)$$

Similarly, we establish a balance equation applied to the interior face of the exterior glass panel and to the exterior face of the interior glass panel:

$$\frac{\lambda_e}{e_e} \cdot (T_{\text{p_ext}} - T_{\text{p_fe}}) = h_{\text{fe}} \cdot (T_{\text{p_fe}} - T_f) - \alpha_{\text{CLO_fe}} \cdot \varphi_{\text{CLO_fe}} - \alpha_{\text{GLO_fe}} \cdot \varphi_{\text{GLO_fe}} \quad (5)$$

$$h_{\text{fi}} \cdot (T_f - T_{\text{p_fi}}) + \alpha_{\text{CLO_fi}} \cdot \varphi_{\text{CLO_fi}} + \alpha_{\text{GLO_fi}} \cdot \varphi_{\text{GLO_fi}} = (T_{\text{p_fi}} - T_{\text{p_i}}) \cdot \frac{\lambda_i}{e_i} \quad (6)$$

$$(T_{\text{p_fi}} - T_{\text{p_i}}) \cdot \frac{\lambda_i}{e_i} = h_{\text{fi}} \cdot (T_{\text{p_i}} - T_{\text{int}}) - \alpha_{\text{CLO_int}} \cdot \varphi_{\text{CLO_int}} - \alpha_{\text{GLO_in}} \cdot \varphi_{\text{GLO_int}} \quad (7)$$

Concerning the air (temperature T_f) contained in the cavity (space within the double skin), we write the following dynamic heat balance:

$$h_{\text{fe}} \cdot (T_{\text{p_fe}} - T_f) - h_{\text{fi}} \cdot (T_f - T_{\text{p_fi}}) = \rho_f \cdot C_p \cdot e_f \cdot \frac{dT_f}{dt} \quad (8)$$

The equations above are gathered in a “module” macro-class. We also created two “interfaces” macro-class for the tips of the double skin, one for the pre-heating phase and the other for the ventilation phase.

Enrichment of the model

Enrichments were brought to the thermal and ventilation basic model. We segmented the air cavity into several “modules”, taking into account the air re-

circulation in the cavity when the double skin is closed (positive and negative flows). We then evaluated the convection coefficients for the ventilated and non-ventilated air cavity. The integration of these modifications in the basic model allowed to improve it.

Segmentation of the air cavity into several “modules”

The main advantage of this segmentation of the height of the wall element lies in the possibility of:

- allotting different glazings characteristics (electrochromic glazing) for the interior and exterior glass panels
- appreciating the thermal stratification within the air cavity
- considering the air re-circulation in the closed air cavity.

We also created an “interface” macro-class that allows to ensure continuity between two “modules”: it contains equations for mass and exchanges. The equations ensuring the connection of “modules” are those used in the interfaces of zonal models proposed by Marjorie Musy [Musy, 2001]. We note that “modules” represent the parallelepiped-shaped zones (Figure 9), and “interface” is the rectangular surface that separates adjacent “modules”. By assembling the appropriate “modules”, we build the global double skin balance.

Otherwise, this model requires to use empirical relations defining the air flows in an air cavity. Very few configurations were studied. Moreover, the required relations are valid only for one precise configuration because the convection movements in the air cavity depend on the temperature difference, the cavity form ratio and the glazing emissivity... So, the airflow pattern and velocities can vary. We used Betts research [Betts, 2000], which indicates the numerical values of air movement speed in a rectangular cavity with a form ratio (A) of about 28.6.

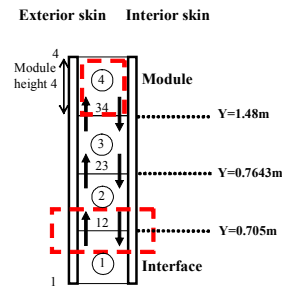


Figure 9: Schematization of various “modules” heights of double skin for December 21 from 3pm to 4pm.

This form ratio is equivalent to the form ratio of our wall element when the air cavity width is about 10cm. We started from Betts results and measurements to

establish an equation expressing the air flow rate in the air cavity according to two values of Rayleigh number ($Ra=0.86 \times 10^6$ and $Ra=1.43 \times 10^6$) for the Y various altitude values in the wall (Figure 10 and Figure 11). From these results, we looked for a relation between the re-circulation flow at a given height and the Rayleigh number. The two following equations expressing the flow rate according to the Rayleigh number were implemented into the model.

For $Y=0.705m$ and $Y=0.7643m$:

$$Q(\text{Ray}) = -2.67 \times 10^{-16} Ra^2 + 3.71 \times 10^{-9} Ra \quad (9)$$

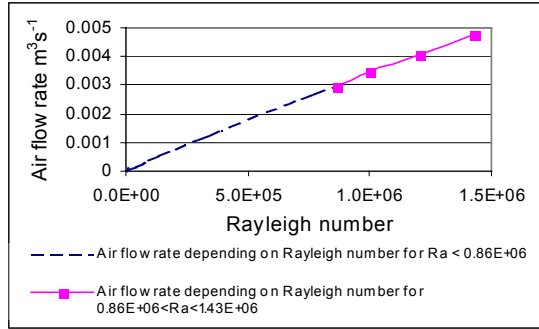


Figure 10: Airflow rate depending on Rayleigh number for $Y=0.705m$ and $Y=0.7643m$.

For $Y=1.48m$:

$$Q(\text{Ray}) = -3.20 \times 10^{-15} Ra^2 + 7.70 \times 10^{-9} Ra \quad (10)$$

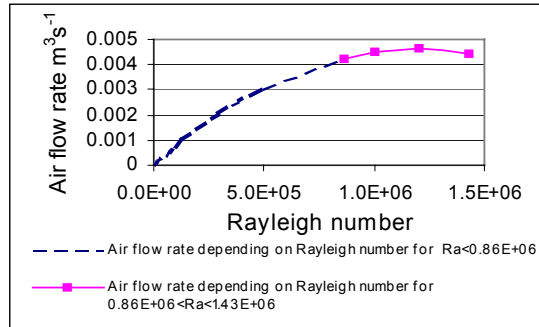


Figure 11: Airflow rate depending on Rayleigh number for $Y=1.48m$.

Convective heat transfer coefficients refinement

A preliminary study comparing the various methods to evaluate the convective heat transfer coefficient (hc) highlighted the difficulty and the importance to choose the method calculation corresponding to the considered air cavity configuration because each method is valid only for one precise configuration. We retained the coefficient hc calculation method (for a non-ventilated air cavity) proposed in the ISO/15099 norm which constitutes the future International ISO standard: The standard proposes to calculate two values of the Nusselt number (Nu), one which takes into account only the Rayleigh value and the other which takes into account the cavity form ratio (A). The selected Nusselt number corresponds to the value maximum between Nu_1 and Nu_2 :

$$Nu_1 = 0.0673838 Ra^{1/3} \text{ for } 5 \times 10^4 < Ra < 10^6 \quad (11) \text{ WRIGHT}$$

$$Nu_1 = 0.028157 Ra^{0.4134} \text{ for } 10^4 < Ra < 5 \times 10^4 \quad (12) \text{ WRIGHT}$$

$$Nu_1 = 1 + 1.7596678 \times 10^{-10} Ra^{2.2984755} \text{ for } Ra \leq 10^4 \quad (13)$$

WRIGHT

$$Nu_2 = 0.242 \cdot \left[\frac{Ra}{A} \right]^{0.272} \quad (14) \text{ ELSHERBINY}$$

$$\text{with, } Ra = \frac{\rho^2 \cdot d^3 \cdot g \cdot \beta \cdot C_p \cdot \Delta T}{\mu \cdot \lambda} \quad (15)$$

$$\text{Then } hc = Nu \left(\frac{\lambda}{d} \right) \quad (16)$$

We also retained this ISO/DIS 15099 standard to define the convective heat transfer coefficient values when the air cavity is ventilated. The convection coefficient value for a ventilated air cavity was calculated from the convection coefficient value for a non-ventilated air cavity and from air velocity according to :

$$hc_v = 2hc + 4v \quad (17) \quad v = \frac{\dot{V}}{eI} \quad (18)$$

The equations allowing to calculate the convection coefficients in the case of a ventilated or non-ventilated air cavity have been introduced into the model.

Optimization of the envelope thermal performances

The thermal efficiency criterion we choose corresponds to the calculation of the power recovered by this device as follows :

$$P = \phi_{\text{haut}} - \phi_{\text{bas}} + \phi_{\text{transmis_dv1}} + \phi_{\text{transmis_dv2}} + \phi_{\text{transmis_dv3}} + \phi_{\text{transmis_dv4}} \quad (19)$$

The transmitted flux (ϕ_{transmis}) is the one transmitted through the double skin (conduction in the wall element added to transmitted short-wave radiative flux). The expression ($\phi_{\text{haut}} - \phi_{\text{bas}}$) corresponds to the air pre-heating in the cavity. This efficiency criterion also allowed us to carry out the choice of ventilation scenario for the fall/winter period (pre-heating phase and ventilation phase) and the choice of glazing configuration.

Choice of ventilation scenarios (fall/winter)

Three extreme ventilation scenarios were tested: $t_{ch}/t_{vid} = 1$, $t_{ch}/t_{vid} = 1/3$ and $t_{ch}/t_{vid} = 3$. The ventilation phase (t_{vid}) was chosen so that the air cavity be totally drained and so that the hygienic flow rate be respected according to equation (1) and to the following relation:

$$t_{vid} = \frac{V_f}{Q_{vid}} = \frac{3 \times 2.5 \times e}{Q_{vid}} \quad (20)$$

For the scenario choice simulations, we considered a glazing configuration, named A (exterior glazing ($\tau_{\text{maxi}} 71$, $\rho_{\text{maxi}} 7$, α) and interior glazing ($\tau_{\text{mini}} 25$,

ρ , $\alpha_{\max i}$ 57). Figure 12 and Table 1 show the calculation results.

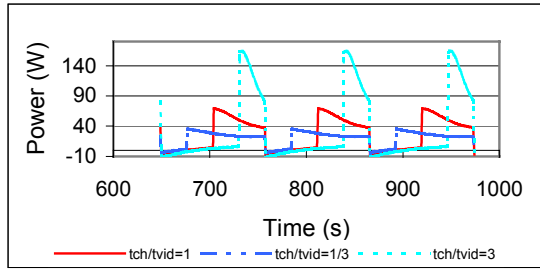


Figure 12: Choice of ventilation scenario configuration depending on the mean power through the air cavity (fall/winter).

The mean power recovered by the device is made on one cycle applying the following relation:

$$\Sigma P \times dt / t_{\text{cycle}} \quad (21)$$

Table 1: Scenario choice (fall/winter): mean recovered power (W) through the air cavity with glazing configuration A.

	Scenario choice: mean recovered power (W) through the air cavity with glazings configuration A
$t_{\text{ch}}/t_{\text{vid}}=1$	25,9
$t_{\text{ch}}/t_{\text{vid}}=1/3$	19,8
$t_{\text{ch}}/t_{\text{vid}}=3$	31,2

The results indicate that for a 10cm air cavity, the ventilation scenario allowing to recover the maximum energy through the wall element corresponds to the configuration $t_{\text{ch}}/t_{\text{vid}}=3$. We could test greater ratios to determine an optimum. However, the increase of $t_{\text{ch}}/t_{\text{vid}}$ implies a flow increase during the ventilation period (Equation 1). Therefore, more important openings areas to make natural ventilation are necessary. A compromise for the device dimensioning should be found.

Choice of glazings configurations

To answer to the climatic constraints, to optimize the wall element and to determine the main tendencies, we selected interior/exterior glazings combinations taking extreme and medium values of transmission, reflection and absorption coefficients.

A configuration: exterior glazing ($\tau_{\max i}$ 71, $\rho_{\max i}$ 7, α) and interior glazing ($\tau_{\min i}$ 25, ρ , $\alpha_{\max i}$ 57)

B configuration: exterior glazing (τ ; $\rho_{\min i}$ 15; $\alpha_{\max i}$ 48) and interior glazing ($\tau_{\max i}$ 46; $\rho_{\max i}$ 22; α)

C configuration: exterior glazing ($\tau_{\max i}$ 71, $\rho_{\max i}$ 7, α) and interior glazing (τ_{mean} 37, ρ_{mean} 27, α_{mean} 37)

D configuration: exterior glazing (τ ; $\rho_{\min i}$ 15; $\alpha_{\max i}$ 48) and interior glazing (τ_{mean} 36, ρ_{mean} 27, α_{mean} 37)

The simulations were carried out with the SPARK dimensioning tool.

For a 10cm air cavity, the configuration that allows recovering the maximum of energy through the wall element (Figure 13 and Table 2) corresponds to the A configuration (Glazing of the exterior wall: $\tau=71$; $\rho_e=7$; $\rho_i=7$;

$\alpha_e=22$ ($\tau_{\max i}$, $\rho_{\max i}$, α), Glazing of the interior wall: $\tau=25$; $\rho_e=18$; $\alpha_e1=48$; $-\alpha_e2=9$ ($\tau_{\min i}$, ρ , $\alpha_{\max i}$)).

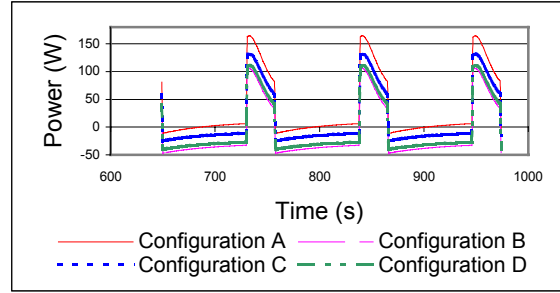


Figure 13: Choice of glazings configuration depending on the mean power through the air cavity.

Table 2: Choice of glazings configuration: mean recovered power (W) through the air cavity.

	Choice of glazings configuration: mean recovered power (W) through the air cavity
Configuration A	31,7
Configuration B	-10,5
Configuration C	12,6
Configuration D	4,1

Proportion of the flux transmitted through the wall element by conduction, radiation or recovered by air cavity pre-heating

The proportion of the flux transmitted through the wall element by conduction, radiation and the proportion of the flux recovered by the pre-heating of the air contained in the cavity are compared to the total flux for the three ventilation scenarios with the A glazings configuration. Among the three ventilation scenario configurations, the one that allows to limit the heat losses through the envelope corresponds to the scenario $t_{\text{ch}}/t_{\text{vid}}=3$ (Figure 14).

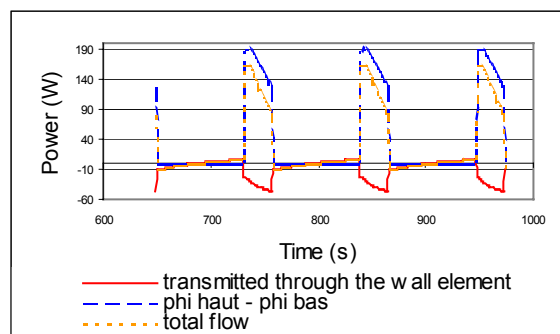


Figure 14: Proportion of the flux transmitted through the wall element by conduction, radiation and proportion of the flux recovered by air cavity pre-heating for the A configuration and $t_{\text{ch}}/t_{\text{vid}}=3$.

The energy recovered by the wall element with the A glazings configuration comes mainly from the air pre-heating. We note losses by conduction through the envelope, this being due to the fact that the air temperature in the air cavity is always lower than the office cell inner temperature.

Devices dimensioning for natural ventilation

The equations allowing for the dimensioning of the ventilation device (in the natural ventilation mode) were also inserted into the equations model. This improvement enabled us to determine the ventilation areas of the ventilation systems.

Loop Equation method

We used the research of Axley [Axley, 2000] who developed a pre-dimensioning method for devices working in natural ventilation. For this purpose, he proposed an equation called the Loop equation writing :

$$\Delta P_v + \Delta P_c = \Sigma \Delta P_{duct} + \Sigma \Delta P_{adapt_duct} + \Sigma \Delta P_{opening} \quad (22)$$

The relation between the pressure difference and the push force (chimney stack effect) is:

$$\Delta P_c = (\rho_o - \rho_i) g \Delta Z \quad (23)$$

The pressure difference related to the wind forces (wind effect) is :

$$\Delta P_v = (C_{p-v} - C_{p-sv}) \rho U_{ref}^2 / 2 \quad (24)$$

The equations related to the pressure loss in a duct, a duct adaptator and an opening, are respectively:

$$\Delta P = \frac{f L \dot{V}^{1/n}}{2 \rho D A^2} \quad (25)$$

$$\Delta P = \frac{C_v \dot{V}^{1/n}}{2 \rho A^2} \quad (26)$$

$$\Delta P = \frac{\dot{V}^{1/n}}{2 \rho C_d^2 A^2} \quad (27)$$

The pressure difference ΔP occurring through the building frontage by the wind and a push force is the basic principle of natural ventilation. The pressure coefficients C_p , which depends on the building geometry, the nature of the environmental obstacles and the direction and the speed of the wind, characterize the wind forces. Then, the temperature difference and the height difference between the air inlet and exhaust air create a buoyancy effect.

Loop equation : Application for the wall element in fall/winter

The “fall/winter” ventilation problem is characterized by a loop equation comprising two ducts and four adaptator ducts. So for the “fall/winter” Loop equation:

$$\Delta P_v + \Delta P_c = \Delta P_{duct1} + \Delta P_{duct2} + \Delta P_{adapt_duct1} + \Delta P_{adapt_duct2} + \Delta P_{adapt_duct3} + \Delta P_{adapt_duct4} \quad (28)$$

Loop equation : Application for the wall element in spring/summer

The “spring/summer” ventilation problem has two loops, a loop which corresponds to the office cell

ventilation and another one which corresponds to the double skin ventilation. The “office cell” loop includes an opening, two adaptator ducts and a duct. So, for the “spring/summer office cell” we have the Loop equation: (29)

$$\Delta P_v + \Delta P_c = \Delta P_{opening1} + \Delta P_{duct1} + \Delta P_{adapt_duct1} + \Delta P_{adapt_duct2}$$

The loop “ spring/summer wall element” has two adaptator ducts and a duct. So, for the “spring/summer wall element” the Loop equation is :

$$\Delta P_v + \Delta P_c = \Delta P_{duct1} + \Delta P_{adapt_conduct1} + \Delta P_{adapt_duct2} \quad (30)$$

The insertion of the these last Loop equations (one for fall/winter and the other for spring/summer) will enable us to size up the ventilation areas of the various components so as to ensure the hygienic flow rate fixed by the regulation, taking into account the pre-heating of air in the cavity.

CONCLUSIONS

We have shown how the SVR interface allowed us to optimize the sizing up of the different architectural elements of the glazing envelope of an office cell façade: shape of the slats and electrochromic protection located in that area devoid of strips. In addition, we have checked the influence of such an optimization on luminous comfort with the Solene software. It has been shown that the thermo-aerologic model and its improvements enabled us to optimize the wall elements design: choice of ventilation scenarios configuration, choice of glazings configuration, evaluation of the proportion of the heat flux transmitted by conduction, radiation through the wall element or recovered by the pre-heating air cavity. The writing of our problem is general and can be used for similar problems since this environment consists in assembling library objects. However, the models used are in general based on empirical laws, which can limits the tools applications. It is then important to undertake experimental studies to fulfill the lack of empirical relations and enrich these simplified models and also to validate them. From the wall element draft, the various tools used (SVR, Solene and SPARK) allowed us to refine the envelope design so as to guarantee comfort conditions to the office occupant. The optimization of the various envelope elements contribute to limit the energy consumption (optimal use of the daylighting, losses limitation through the wall element thanks to the air cavity pre-heating).

We wanted also to show that tools such as SVR, and as the present developed model are particularly adapted for the use by architects. In effect, not only are these models user-friendly (no formal training is needed) and cheap, but they allow to reach a high degree of performance determinations for architect-designed elements. In particular, SVR could be

largely used by French architectural agencies since it is accessible through Autocad 2000®.

ACKNOWLEDGEMENTS

The authors gratefully acknowledge the financial support provided by ADEME for this Ph.D. research.

REFERENCES

- Axley, J. W, "Design and simulation of natural ventilation systems using Loop Equations", Healthy Building 2000, Helsinki, Finland, 2000.
- Betts, P.L. and I.H. Bokhari, "Experiments on Turbulent Natural Convection in an enclosed tall cavity", Int. J. Heat And Fluid Flow, 2000.
- Groleau, D., "Solene un outil de simulation des éclairagements solaires et lumineux dans les projets architecturaux et urbains", in "Les professionnels de la construction la construction, confort interieur": outils informatiques d'aide à la conception et à la prévision du contrôle thermique, acoustique et d'éclairage, Etude de cas, 2000.
- Houpert, S. "SVR, a software to solve solar constraints, a help to better take into account architectural environmental and ecological problems", PLEA 2002, Toulouse, France 2002.
- Lawrence Berkley Laboratory, "Visual SPARK user's guide – Simulation problem and analysis research Kernel", 1997-2001.
- Meunier, V., "Elément de façade multicritère", 1^{ère} journée d'étude en Lorraine sur le matériau verre, Nancy, France, 2001.
- Meunier, V. and S. Houpert, R. Brec, "Optimization of a sunbreaker envelope from an CAD software inverse approach", EPIC 2002 / AIVC, Lyon, France, 2002.
- Musy, M. and E. Wurtz, F. Winkelmann, F. Allard, "Generation of a zonal model to simulate natural convection in a room with a radiative/convective heater", Building and Environment 36, 2001.
- Musy, M. and F. Winkelmann, E. Wurtz, A. Sergent, "Automatically generated zonal models for building airflow simulation: principles and applications", Building and Environment 37, 2002.

NOMENCLATURE

- A: surface area, m²
- C: pressure loss coefficient
- Cd: discharge coefficient
- Cp: specific heat of air, J kg⁻¹ K⁻¹
- Cp: wind pressure coefficient
- d: width, m

- D: hydraulic diameter, m
 - e: thickness, m
 - Ei: incident daylighting, W m⁻²
 - f: friction factor
 - g: gravitational acceleration, m s⁻²
 - h: height, m
 - hc: convective heat transfer coefficient, W m²K⁻¹
 - l: length, m
 - n: exponent defining the flow type
 - Nu: Nusselt number
 - Q: Airflow rate, kg s⁻¹
 - Ra: rayleigh number
 - t: time, s
 - T: temperature, K
 - Tp: wall temperature, K
 - Uref: reference wind speed, m s⁻¹
 - v: average speed, m s⁻¹
 - V: volume, m³
 - \dot{V} : volumic flow rate, m³ s⁻¹
 - α : absorption coefficient
 - β : coefficient of thermal expansion, K⁻¹
 - λ : air thermal conductivity, W m⁻¹
 - μ : dynamic viscosity, Pa.s
 - ρ : air density, kg³ m⁻³
 - ϕ : heat flux, W m⁻²
 - ΔP : pressure difference, Pa
 - ΔT : temperature difference, K
- Index / Exponent
- ch: relating to the pre-heating of the air cavity
 - cycle: relating to the cycle (t_{ch}+t_{vid})
 - CLO: relating to the short wavelengths radiation
 - e: exterior wall
 - ext: outside
 - i: interior wall
 - int: inside
 - f: relating to the air cavity
 - fe: relating to interior surface of exterior wall
 - fi: relating to exterior surface of interior wall
 - GLO: relating to the long wavelengths radiation
 - hyg: hygienic
 - sv: "leeward"
 - v: "windward"
 - vid: relating to the ventilation phase of the air cavity